Tamed Frequency Modulation, A Novel Method to Achieve Spectrum Economy in Digital Transmission

FRANK de JAGER AND CORNELIS B. DEKKER, MEMBER, IEEE

Abstract—**This paper describes a new type of frequency modulation, called Tamed Frequency Modulation (TFM), for digital transmission. The desired constraint of a constant envelope signal is combined with a maximum of spectrum economy which is of great importance, particularly in radio channels. The out-of-band radiation is substantially less as compared with other known constant envelope modulation techniques. With synchronous detection, a penalty of only 1 dB in error performance is encountered as compared with four-phase modulation. The idea behind TFM is the proper control of the frequency of the transmitter oscillator, such that the phase of the modulated signal becomes a smooth function of time with correlative properties. Simple and flexible implementation schemes are described.**

I. INTRODUCTION

In the last fifteen years numerous modulation systems for efficient digital transmission via telephone lines have been introduced. In almost all cases the resultant modulated signals exhibit amplitude variations. Such systems are implemented with linear amplifiers and linear modulators. For radio communication constant-envelope modulated signals are preferable due to existing system constraints in power economy and the consequent use of non-linear power amplifiers. Quite naturally this leads to the use of frequency modulation.

However, the spectrum of an FM signal is relatively wide. In order to narrow the spectrum, a channel filter with a precisely prescribed attenuation and phase characteristic may be used but this is not attractive in radio equipment. Besides, a filter of this kind cannot be used if the transmitted center frequency has to be changed.

Another method for narrowing the spectrum is to shape the data at the input of the frequency modulator by means of a filter. The requirements to be met by this premodulation filter are manifold. The use of the filter has to result in a transmitted spectrum which is as narrow as possible in order to be efficient with regard to spectrum economy. We may, in addition, require that the receiver has to be able to detect the signal reliably, even with an unknown frequency shift between the transmitter and the receiver. Moreover, if an orthogonal coherent demodulator is used, the detection should in principle be independent of the level of the received signal.

A solution to these problems, called Tamed Frequency Modulation (TFM), is described in the present paper. The concept of TFM is explained in the first section. In the next section we calculate the necessary transfer characteristic of the premodulation filter. In the following section the influence of some parameters of the transfer characteristic on the TFM spectrum will be investigated. The description of the receiver and the calculation of the receiving filters follows next. It will then be shown that the implementation can be simple and flexible. The last section presents a further evaluation to obtain other types of synchronous frequency modulation.

Manuscript received October 7, 1977.

The authors are with Philips Research Laboratories, Eindhoven, The Netherlands.

II. THE CONCEPT OF TFM

To start with, we will consider four-phase modulation (4ϕ), well known from digital transmission via telephone lines. With this modulation method information can be transmitted efficiently in a relatively narrow bandwidth. In the two-dimensional representation of its signal space diagram in Fig. 1(a), four signal points are defined on a circle. Every two bits of the incoming binary data stream are encoded into one of these points. Between two sampling moments, the phasor $v(t)$, representing the modulation, moves from one point to another. The way in which this takes place determines the spectrum width of the modulated signal. The magnitude of the phasor is often deliberately not kept constant between the sampling moments, in order to reduce the spectrum width. However, as mentioned in the introduction, we prefer a constant amplitude for our communication applications.

The coherent orthogonal demodulator is the optimum receiver structure for 4ϕ-modulation [1]. A certain frequency shift between the transmitter and the receiver can be tolerated because a carrier recovery system is used. Detection depends only on the polarity of the X and Y components of the incoming signal. Some of the conditions mentioned in the introduction are thus automatically fulfilled.

In order to avoid amplitude variations the phasor $v(t)$ must remain on a circle during the transitions from one signal point to another. An example of a system with this performance is frequency shift keying with a modulation index $m = 0.5$ [2], also called Fast Frequency Shift Keying (FFSK) [3] or Minimum Shift Keying (MSK) [4], whose signal space diagram is given in Fig. 1(b). During a sampling interval the phasor moves from a signal point to one of the two neighboring ones. The corresponding variation of the phase $\phi(t)$ of the modulated signal is indicated by the dashed line in Fig. 2. However, the power spectral density function (PSDF) [5] of MSK, represented by the dashed line in Fig. 3, is somewhat wide.

This is mainly due to the sharp edges in the phase path. The spectrum will be narrowed if the edges are smoothed and coherent detection remains possible if the phase values remain the same at the sampling moments, $t = mT$ (m integer and $T = 1/f_{bit} = 2\pi/\omega_{bit}$).

0090-6778/78/0500-0534$00.75

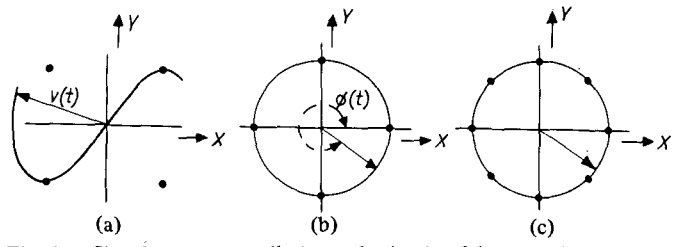

Fig. 1. Signal space constellations of a 4ϕ-signal (a), an MSK signal (b) and a TFM signal (c).

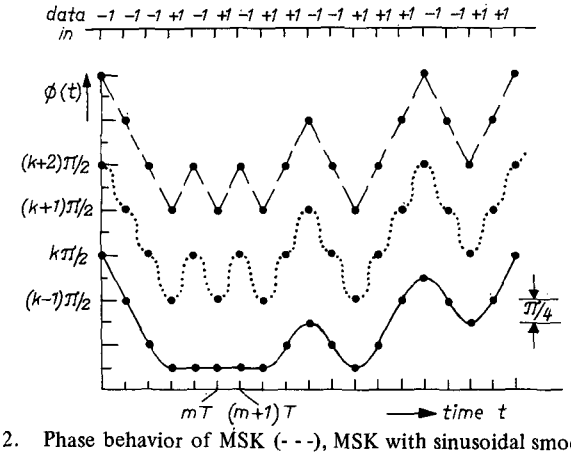

Fig. 2. Phase behavior of MSK (- - -), MSK with sinusoidal smoothing (· · · ·) and TFM (——).

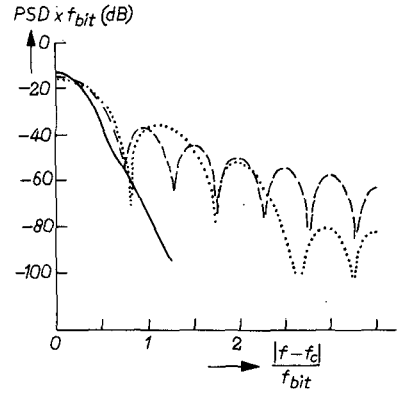

Fig. 3. Power spectral density functions of MSK (- - -), MSK with sinusoidal smoothing (· · · ·) and TFM (——).

In the literature considerable attention has been devoted to finding the optimal smoothing, in the sense of giving a PSDF which is as narrow as possible. Amoroso [4] used the sinusoidal smoothing represented by the dotted line in Fig. 2. The sharp edges have disappeared but the maximum slope of the phase path has considerably increased. The corresponding PSDF, given in Fig. 3 by the dotted line, therefore shows but little improvement.

We found that it is possible to obtain a considerably better spectrum efficiency by prescribing a phase path as depicted by the solid line in Fig. 2. We named this modulation method Tamed Frequency Modulation (TFM). The phase path is characterized by the fact that the values of the phase at the successive sampling moments $t = (m-1)T, mT, (m+1)T, \cdots$ are obtained from the data via a different code rule from that for MSK. If the data signal $a(t)$ is defined by

$$a(t) = \sum_{n=-\infty}^{\infty} a_n \cdot \delta(t - nT), \qquad \text{with } a_n = +1 \text{ or } -1, \quad (1)$$

then for MSK

$$\phi(mT + T) - \phi(mT) = (\pi/2) \cdot a_m \quad (2)$$

and for TFM

$$\phi(mT + T) - \phi(mT) = (\pi/2) \cdot (a_{m-1}/4 + a_m/2 + a_{m+1}/4) \quad (3)$$

with $\phi(0) = 0$ if $a_0 \cdot a_1 = 1$ and $\phi(0) = \pi/4$ if $a_0 \cdot a_1 = -1$.

From this code rule it is easily established that phase-changes of $\pi/2$ are obtained if three succeeding bits have the same polarity, and the phase remains constant for three bits of alternating polarity. Phase changes of $\pi/4$ are connected with the bit configurations ++−, +−−, −++ and −−+.

In addition the phase should vary as smoothly as possible in going through the values obtained with (3), as shown in Fig. 2. The signal space diagram of TFM is shown in Fig. 1(c). The Tamed Frequency Modulation should not be mixed up with eight-phase modulation, because the phase values of the TFM signal at successive sampling moments are dependent. For example, it is possible only to obtain a constant phase for phase values which are odd multiples of $\pi/4$.

III. SPECIFICATION OF THE PREMODULATION FILTER

The wanted fluctuations of the phase as a function of time are obtained when the signal is applied to a frequency modulator as shown in Fig. 4. The premodulation filter $G(\omega)$ has to shape the data signal $a(t)$ so as to obtain the wanted smooth phase fluctuations. Let the deviation sensitivity of the modulator be K_0 radians/volt/second. With the definition of $a(t)$ in (1) and the impulse response $g(t)$ of the filter, the phase $\phi(t)$ can be written as

$$\phi(t) = K_0 \cdot \int_{-\infty}^{t} \left[\sum_{n=-\infty}^{\infty} a_n \cdot g(\tau - nT) \right] \cdot d\tau + C,$$

or

$$\phi(t) = K_0 \cdot \sum_{n=-\infty}^{\infty} a_n \cdot x(t - nT) + C, \quad (4)$$

where

$$x(t) = \int_{-\infty}^{t} g(\tau) \cdot d\tau$$

and C is a constant. At the sampling moment $t = mT$ the phase becomes

$$\phi(mT) = K_0 \cdot \sum_{n=-\infty}^{\infty} a_n \cdot x(mT - nT) + C$$

and

$$\phi(mT + T) - \phi(mT)$$

$$= K_0 \cdot \sum_{n=-\infty}^{\infty} a_n \cdot [x(mT + T - nT) - x(mT - nT)]$$

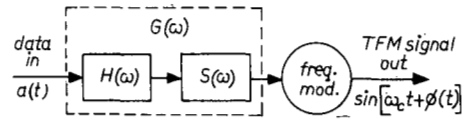

Fig. 4. Basic circuit for the generation of a TFM signal.

or

$$\phi(mT+T)-\phi(mT) = K_0 \sum_{l=-\infty}^{\infty} a_{m-l}\,[x(lT+T)-x(lT)]. \tag{5}$$

From eq. 3 it can be seen that the right-hand side of (5) can be equal to $\pm\pi/2$, $\pm\pi/4$ or 0 radians.

Writing the code rule in (3) in more detail as

$$\phi(mT+T)-\phi(mT) = (\pi/2)\cdot(\cdots + a_{m-2}\cdot 0 + a_{m-1}/4 + a_m/2 + a_{m+1}/4 + a_{m+2}\cdot 0 + \cdots), \tag{6}$$

then, with (5), we obtain

$$x(lT+T)-x(lT) = \begin{cases} \pi/(8K_0) & \text{for } l=1,\\ \pi/(4K_0) & \text{for } l=0,\\ \pi/(8K_0) & \text{for } l=-1,\\ 0 & \text{otherwise.}\end{cases} \tag{7}$$

Combining this with the definition of $x(t)$ in (4) we obtain

$$\int_{lT}^{(l+1)T} g(t)\cdot dt = \begin{cases} \pi/(8K_0) & \text{for } |l|=1,\\ \pi/(4K_0) & \text{for } l=0,\\ 0 & \text{otherwise.}\end{cases} \tag{8}$$

The relation in (8) gives the condition for the impulse response $g(t)$ needed to ensure that the phase goes through the values at the sampling moments shown in Fig. 2 for TFM. This condition is certainly fulfilled if $g(t)$ is derived from a single pulse $h(t)$, satisfying the third Nyquist criterion* [6], [7] by simple scaling and delay operations with a network $S(\omega)$ as is shown in Fig. 5. The transfer characteristic of this network is given by

$$S(\omega) = [\pi/(8K_0)]\cdot e^{-j\omega T} + [\pi/(4K_0)] + [\pi/(8K_0)]\cdot e^{j\omega T} = [\pi/(2K_0)]\cdot\cos^2(\omega T/2). \tag{9}$$

* An impulse response $h(t)$ satisfies the third Nyquist criterion if, for any integer l:

$$\int_{(2l-1)\cdot T/2}^{(2l+1)\cdot T/2} h(t)\,dt = \begin{cases} 1 & \text{for } l=0,\\ 0 & \text{otherwise.}\end{cases}$$

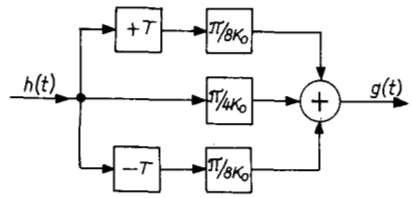

Fig. 5. Network with a transfer characteristic $S(\omega) = [\pi\cos^2(\omega T/2)]/(2K_0)$.

The overall shape factor $G(\omega)$ of the premodulation filter can now be written as

$$G(\omega) = H(\omega)\cdot S(\omega) = [\pi/(2K_0)]\cdot H(\omega)\cdot\cos^2(\omega T/2) \tag{10}$$

where $H(\omega)$ applies to any filter giving a pulse satisfying the third Nyquist criterion.

IV. DIFFERENT TFM SYSTEMS

In the previous sections we have seen that the combination of a premodulation filter $G(\omega)$, defined in (10), and a frequency modulator with deviation sensitivity K_0, gives rise to a phase behavior as given in (5), thus yielding a TFM system. The filter $S(\omega)$, being a part of $G(\omega)$, determines the total amount of phase increase or decrease during a sampling interval, while the other part of $G(\omega)$, namely $H(\omega)$, prescribes the phase path from $\phi(mT)$ to $\phi(mT+T)$. In this section we will look at the influence of different functions for $H(\omega)$ on the TFM spectrum.

Generally, $H(\omega)$ can be written as [7]:

$$H(\omega) = [(\omega T)/(2\sin(\omega T/2))]\cdot N_1(\omega), \tag{11}$$

where $N_1(\omega)$ is the Fourier spectrum of a function satisfying the first Nyquist criterion. A class of Nyquist characteristics which has been extensively used and studied is the raised-cosine characteristic [1]:

$$N_1(\omega) = \begin{cases} 1 & \text{for } 0 \leqslant |\omega| \leqslant \pi(1-\alpha)/T,\\ [1-\sin((T\omega-\pi)/2\alpha)]/2 & \\ \quad \text{for } \pi(1-\alpha)/T \leqslant |\omega| \leqslant \pi(1+\alpha)/T, & \\ 0 & \text{otherwise.}\end{cases} \tag{12}$$

The only variable left is the roll-off factor α ($0 \leqslant \alpha \leqslant 1$). For various values of α the PSDF's of the corresponding TFM systems will be calculated.

In following the calculation method of Garrison [5], we truncate the length of the impulse response $g(t)$ of the network $G(\omega)$ to five symbol intervals ($5T$), and we henceforth approximate the impulse response with eight samples per bit interval T. If Garrison's method is applied to a system in which $G(\omega)$ is implemented by analog means, then the results incorporate an approximation error. However, for a digital implementation this error does not occur.

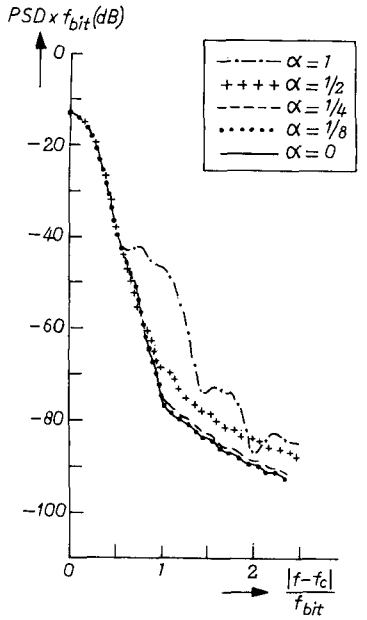

Fig. 6. PSDF's of the TFM signal with different roll-off factors in the transfer characteristic of the premodulation filter.

The resulting power spectral density functions**, plotted in Fig. 6, show no great improvement of the out-of-band radiation when the roll-off factor α is made smaller than 0.25.

A certain truncation of the length of the impulse response $g(t)$ also has to be accepted, so as to keep the amount of hardware for the implementation of $G(\omega)$ small. In the following, the PSDF of TFM is calculated three times for different truncation lengths ($3T$, $5T$, $7T$). For $H(\omega)$ we have chosen a filter with the smallest bandwidth ($\alpha = 0$) [8]:

$$H(\omega) = \begin{cases} \omega T/(2 \sin(\omega T/2)) & \text{for } |\omega| \leqslant \pi/T, \\ 0 \quad \text{otherwise.} \end{cases} \tag{13}$$

The shape factor of $G(\omega)$ with this $H(\omega)$ is

$$G(\omega) = \begin{cases} [\pi\omega T/(4K_0 \cdot \sin(\omega T/2))] \cdot \cos^2(\omega T/2) \\ \quad \text{for } |\omega| \leqslant \pi/T, \\ 0 \quad \text{otherwise} \end{cases} \tag{14}$$

and the corresponding $g(t)$ is shown in Fig. 7. The PSDF's of TFM systems with different truncation lengths of $g(t)$, depicted in Fig. 8, show a considerable reduction of the out-of-band radiation if the length is increased. When we draw the PSDF of the $7T$-version of TFM in Fig. 3 (solid line), we see finally the great improvement obtained by TFM in comparison with MSK and MSK with sinusoidal smoothing.

V. RECEIVER STRUCTURE

From the signal space diagram of TFM in Fig. 1(c) it can be seen that an orthogonal coherent demodulator can be used as

** The 0 dB reference is a constant but arbitrary value throughout the paper.

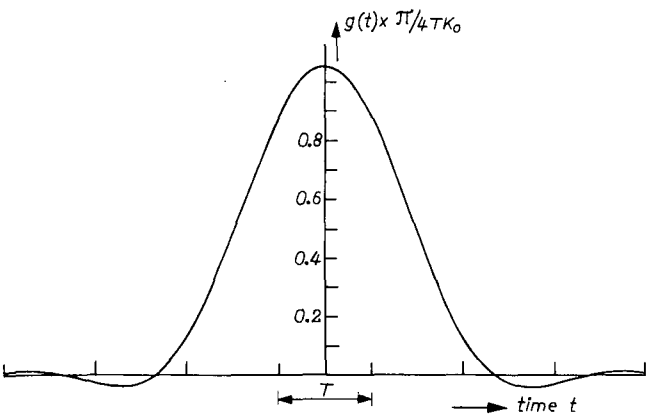

Fig. 7. Impulse response $g(t)$ of the premodulation filter.

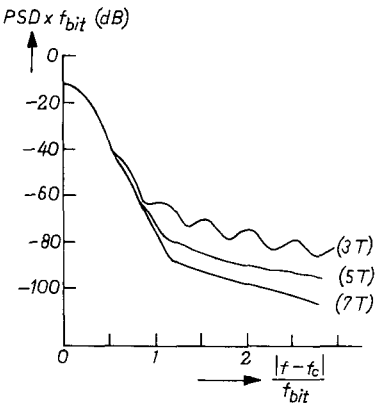

Fig. 8. PSDF's of the TFM signal with different truncations of the length of the impulse response of the premodulation filter.

receiver (Fig. 9). The incoming TFM signal $\sin(\omega_c t + \phi(t))$ is multiplied by respectively $\sin(\omega_c t)$ and $\cos(\omega_c t)$. This results in baseband signals $\cos[\phi(t)]$ and $\sin[\phi(t)]$ which follow from the phase function in Fig. 2. The observed eye patterns are shown in Fig. 10(a) and these signals arrive at the input of the low-pass filters $A_1(\omega)$ and $A_2(\omega)$, together denoted as $A_{1,2}(\omega)$. These filters provide for minimization of the error probability. Finally, a decoder of the same configuration as used by de Buda [3] in his MSK demodulator, can produce the output data signal. In the MSK case, the demodulated signals in de Buda's decoder can only have the amplitude 1 at the sampling moments, while in TFM the amplitude can be 1 or 0.707. This is due to the smoothed phase path occurring in TFM, which however does not affect the polarity of the demodulated signals. This can be shown in a straight-forward way by comparing the phase paths of both FFSK and TFM (Fig. 2).

The deterioration of the eye opening of TFM will cause a somewhat higher error probability, but in this section we will see that the penalty is only 1 dB as compared with 4ϕ-modulation. The question of error propagation and the need for differential encoding for TFM are the same as for MSK [3].

Also, carrier recovery and clock recovery for TFM and MSK are quite similar. We will come back to this in the following section.

The low-pass filters $A_{1,2}(\omega)$ need some special attention. The filters have to minimize the error probability. This can be

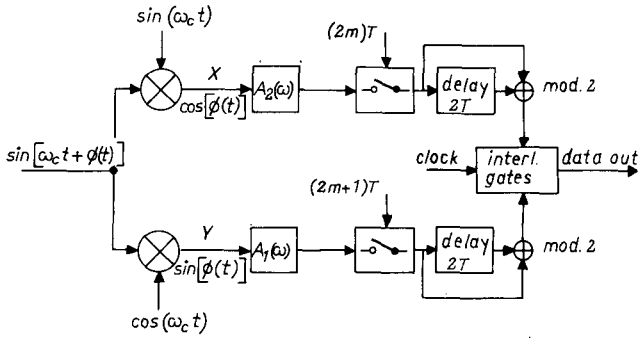

Fig. 9. Orthogonal coherent receiver structure.

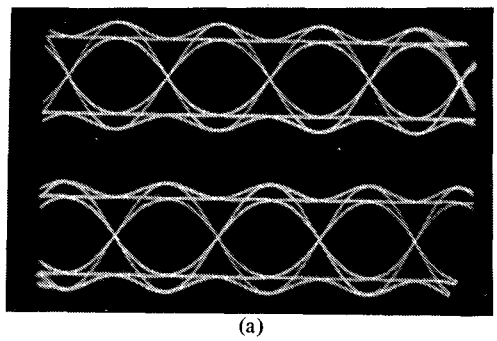

(a)

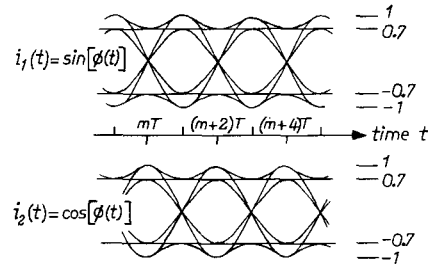

(b)

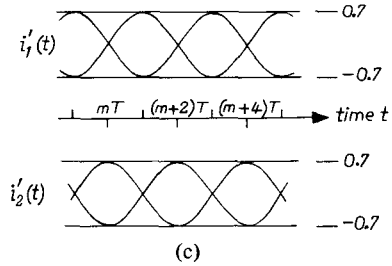

(c)

Fig. 10. Observed eye patterns of the demodulated signals (a, b) and eye patterns of the approximating signals (c).

done by simply minimizing the noise variance σ^2 in the output signal, if the intersymbol interference is taken to be zero. The solution to this problem is described in the following.

If we suppose for the moment that the transfer characteristics from the data input of the transmitter to the inputs of the filters can be regarded to be the transfer characteristics of two linear networks $I_1(\omega)$ and $I_2(\omega)$, then the optimum receiver filters can be found according to Lucky et al. [1]. Since it is not at all obvious that $I_1(\omega)$ and $I_2(\omega)$ for TFM exist and even so, how they should be derived analytically, we make approximating descriptions, which considerably simplifies this problem.

The observed eye patterns of Fig. 10(a) are schematically redrawn in Fig. 10(b). The eye opening at the sampling moment can see to be $\sqrt{2}(\approx 1.4)$. Two slightly different signals $i_1'(t)$ and $i_2'(t)$ with the same opening are shown in Fig. 10(c). These signals can be constructed by superimposing impulse responses $z(t)$, which can be written as:

$$z(t) = \begin{cases} \sqrt{2}[1 + \cos(\pi t/(2T))/4] & \text{for } |t| \leqslant 2T, \\ 0 & \text{otherwise.} \end{cases} \tag{15}$$

Now the linear expressions for $i_1'(t)$ and $i_2'(t)$ can be given as

$$i_1'(t) = \sum_{p=-\infty}^{\infty} v_p \cdot \{z(t - 2Tp)\}, \tag{16a}$$

where $v_p = +1$ or -1, and

$$i_2'(t) = \sum_{p=-\infty}^{\infty} w_p \cdot \{z(t - T - 2Tp)\}, \tag{16b}$$

where $w_p = +1$ or -1.

The corresponding shape factors $I_1'(\omega)$ and $I_2'(\omega)$ are

$$I_1'(\omega) = I_2'(\omega) = I'(\omega) = [\sin(2\omega T)] / [2\omega T(1 - (2\omega T/\pi)^2)]. \tag{17}$$

The power spectral density function $[I'(\omega)]^2$ of the signals in (16a) and (16b) is shown in Fig. 11 and approximates the PSDF, $[I(\omega)]^2$, derived from Fig. 8, of the real input signals. With this $I'(\omega)$ rather than $I_1(\omega)$ and $I_2(\omega)$ a useful, nearly optimum filter $A_1(\omega) = A_2(\omega) = A(\omega)$ can easily be found, leading to the transfer characteristic which is shown in Fig. 12. Its equivalent noise bandwidth ω_r is found to be:

$$\omega_r = \int_0^{\infty} A^2(\omega) \cdot d\omega \approx 0.7\,\pi/T. \tag{18}$$

With this approximate filter the calculated bit error probability is only 1 dB worse for TFM (Fig. 13) in comparison with 4ϕ modulation as calculated by Lucky et al. [1].

In practice the difference will be even smaller because ideal rectangular low-pass filters used by Lucky et al. in their description, are not practically feasible. One final observation has to be made. The foregoing calculation of the filters is based on the assumption of white noise, but in practice the out-of-band radiation of transmitters in neighboring channels has to be added and the total disturbing signal received cannot be interpreted as white noise. If this effect is non-negligible the filter $A(\omega)$ has to be re-optimized.

VI. IMPLEMENTATION

a) Transmitter

In this section we give two different implementation diagrams each having its own advantages and disadvantages. The diagram of the transmitter in Fig. 4 is the basis for the first implementation. In the description of the TFM signal we have

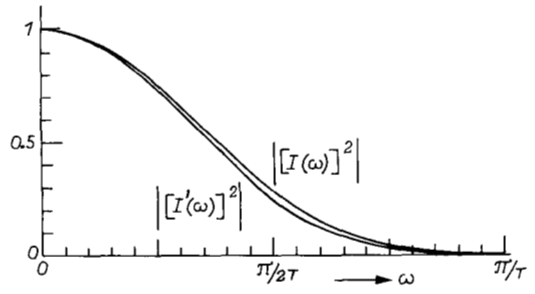

Fig. 11. PSDF's of the demodulated signals and the approximate signals.

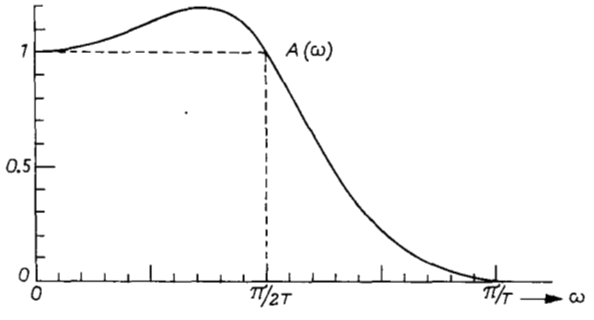

Fig. 12. Transfer characteristic of the low-pass filter $A(\omega)$.

$$P_{4\phi} = \tfrac{1}{2}\operatorname{erfc}(\sqrt{\eta})$$

$$P_{TFM} = \tfrac{1}{4}\operatorname{erfc}(\sqrt{\eta}) + \tfrac{1}{4}\operatorname{erfc}(\sqrt{.69\eta})$$

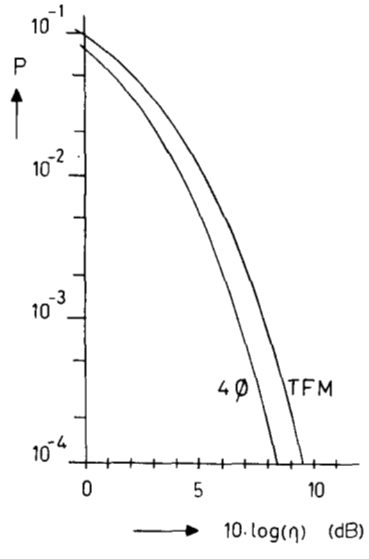

Fig. 13. Error probability curves for 4ϕ modulation and TFM with ideal recovered carrier and clock. The variable η is the signal-to-noise ratio at the input of the receiver in a bandwidth $1/T$.

assumed the center frequency ω_c and the deviation sensitivity K_0 to be invariant. In practice, however, they are insufficiently constant. Extra measures have to be taken, as shown in Fig. 14(a), to keep these parameters at the prescribed values. An adder is inserted for control of the center frequency, while a multiplier can be used to keep the deviation of the frequency modulator at the correct value when K_0 varies. Both are controlled by means of a detector. This circuit has to generate the two control signals to make the phase $\phi(t)$ in the output TFM signal sin $[\omega_c t + \phi(t)]$ pass through the prescribed values at the sampling moments, as shown in Fig. 2. In addition, the

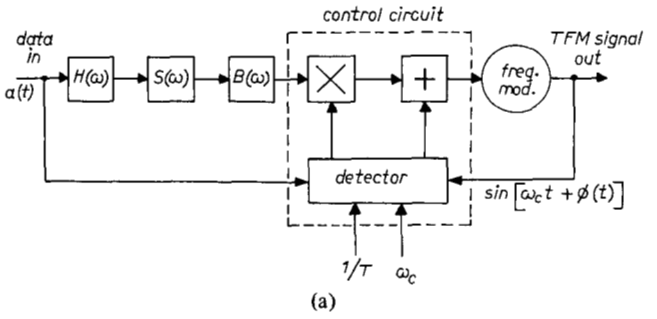

(a)

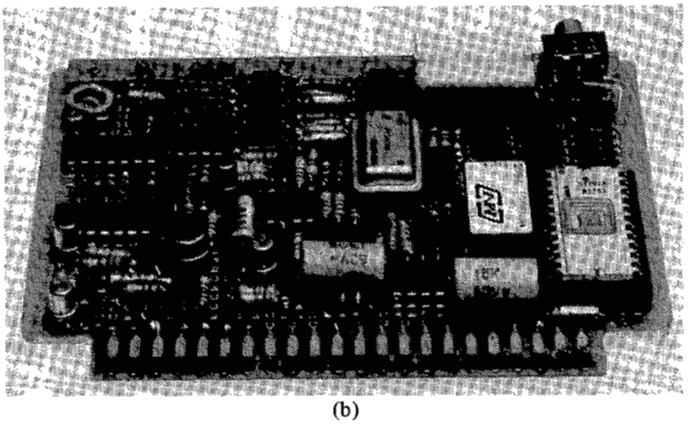

(b)

Fig. 14. Diagram of the TFM transmitter with control circuit (a) and the implementation (b) without the oscillator.

center frequency has to be kept at the specified value. The detector therefore receives as input parameters the input data signal $a(t)$, the sampling moments and the value of the center frequency. These parameters give the information about the center frequency needed and the increase or decrease of the phase per bit interval. The control circuit can be thought of as consisting of two cooperating phase-locked loops. The analytical optimization of this system is difficult since it is a two-dimensional control process.

By combining the filters $H(\omega)$ and $S(\omega)$, the premodulation filter can be easily implemented by means of a digital filter [9]. An extra low-pass filter $B(\omega)$ has to be added to reject spurious signals around multiples of the sampling frequency f_s of the digital filter. Fig. 14(b) shows the implementation of the control circuit and the filters. The advantage of this type of TFM transmitter is that the output TFM signal can exactly meet the constant amplitude condition. A disadvantage is the presence of a feedback system which might cause instabilities.

The other type of transmitter, which is shown in Fig. 15(a), is based on a quadrature modulator. Two signals sin $[\phi(t)]$ and cos $[\phi(t)]$ are fed from a network E to two product modulators operating in quadrature. It will be seen that the output signal is sin $[\omega_c t + \phi(t)]$, i.e., the wanted TFM signal. This signal can thus be applied to a class-C power amplifier, without introducing extra out-of-band radiation. A more detailed implementation diagram is given in Fig. 15(b). The data a_{n+3} enter a shift register with a length of q bits. The value q corresponds with the number of bit intervals to which the length of the impulse response $g(t)$ is truncated ($q \geq 3$), as described in the previous section. For the moment we have taken $q = 5$. From equation 3 it can be seen that the difference in phase

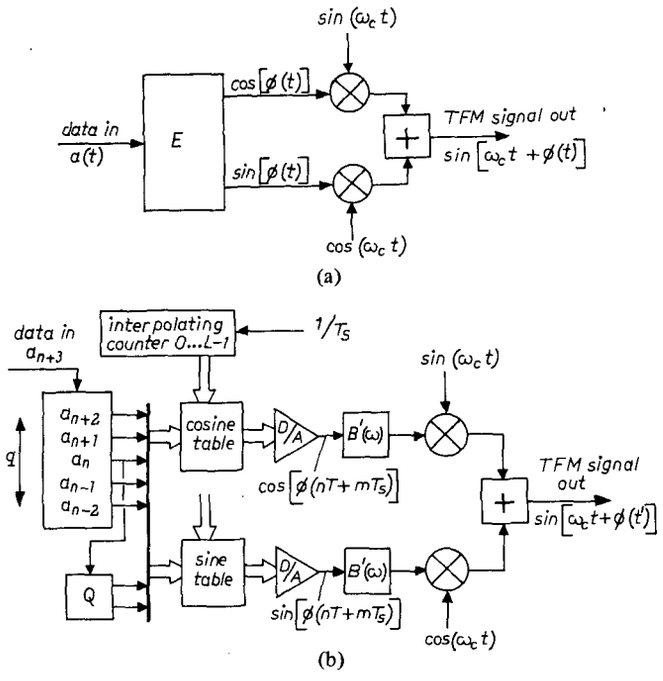

Fig. 15. Basic diagram of the TFM transmitter without a feedback system (a) and a more detailed diagram (b).

between two sampling moments does not exceed $\pm\pi/2$ radians. The cross-over to another quadrant takes place at the sampling moments. Within each quadrant, the phase path is completely determined by the impulse response $g(t)$, truncated over $5T$, and the values a_{n-2}, a_{n-1}, a_n, a_{n+1} and a_{n+2} which are present in the shift register. Moreover, it is necessary to remember in which quadrant the phase path is located. From equation 3 it can be deduced that the phase shifts to a following quadrant in the phase diagram if two successive data symbols have the same value +1. It shifts in the opposite direction if the value is −1. It remains in the original quadrant if the two data symbols do not have the same value. A modified up/down counter, here called quadrant counter Q, can perform this task. The number of the quadrant is represented by two output bits.

The 7 bits, 2 for the quadrant information and 5 for the phase path, form the address for two digital memories called the sine table and the cosine table. The sin $[\phi(t)]$ and cos $[\phi(t)]$, corresponding to the 7 bits, are stored in these memories. The size of the memories increases with q. These "tables" are read out with a sampling frequency f_s. Generally speaking, $f_s = 1/T_s = L \cdot f_{\text{bit}}$, where L is an interpolation factor [10]. The sampled values sin $[\phi(nT + mT_s)]$ and cos $[\phi(nT + mT_s)]$, with $m = 0, 1, 2, \cdots, L - 1$, are supplied via digital-to-analog converters and low-pass filters $B'(\omega)$ to the modulators. The accuracy of the converters is limited. This means that we get some distortion which can be considered as noise. At the moment, the accuracy required of the D/A converters for a certain permissible amount of out-of-band radiation in a neighboring channel has been determined heuristically. The implementation of the digital signal processing part described above is shown in Fig. 16. The accuracy of the D/A converters is eight bits and the interpolation factor $L = 8$.

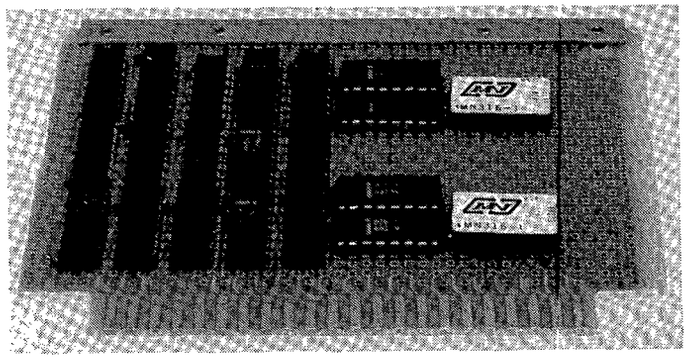

Fig. 16. Implementation of the digital signal processing part E of the TFM transmitter in Fig. 15.

In order to suppress the spurious signals around $\omega_c \pm 2\pi f_s \cdot r$ (r integer) in the modulated signal, low-pass filters $B'(\omega)$ are used. The group delays of these filters should be frequency-invariant and equal in the pass-band. If the cut-off frequency is too low, unwanted variations of the amplitude and phase of the TFM signal will occur. If the interpolation factor L is taken to be large enough, e.g., eight or sixteen, an acceptable cut-off frequency may be $4 \cdot f_{\text{bit}}$ or $8 \cdot f_{\text{bit}}$.

The two parts of the quadrature modulator should have the same flat amplitude and phase characteristic in the frequency band concerned. If they are not the same, amplitude variations and unwanted phase variations will occur, which cannot be eliminated by linear means. For 70 MHz, at which we implemented our TFM system, inequalities of 0.5% have to be taken into account. The power spectral density function measured at the output of the TFM transmitter, shown in Fig. 15 and 16, is given in Fig. 17 and shows good similarity to the corresponding calculated power spectral density function in Fig. 8 ($5T$ version). The flat part in the measured spectrum for $|(f - f_c)/f_{\text{bit}}| > 1$ is caused by the distortion of the 8-bit D/A converters.

The advantage of this type of transmitter is the absence of a feedback system. Its disadvantage is the occurrence of small amplitude variations in practice.

b) Receiver

In the implementation of the receiver according to Fig. 9 a carrier recovery and a clock recovery system have to be provided. These can be similar to the ones suggested by de Buda [3]. The generation of clock and phase reference is based on the fact that the maximal amount of phase change per symbol interval T for both TFM and MSK equals $\pm\pi/2$ radians. Using a frequency doubling circuit, two discrete frequencies are generated. The difference of the frequencies corresponds to the clock frequency and the sum corresponds to four times the carrier frequency.

VII. FURTHER EVALUATION

In the previous sections we have seen that the use of a system according to Fig. 4, where the premodulation filter is defined by $G(\omega) = H(\omega) \cdot S(\omega) = [\pi/(2K_0)] \cdot H(\omega) \cdot \cos^2(\omega T/2)$, gives rise to a TFM signal. The influence of dif-

TABLE 1

$H(\omega)$	$S(\omega)$		
	$\pi/(2K_0)$	$[\pi \cos(\omega T/2)]/(2K_0)$	$[\pi \cos^2(\omega T/2)]/(2K_0)$
$\frac{\sin(\omega T/2)}{\omega T/2}$	(a) Fast Freq. Shift Keying	(b) Duobinary Freq. Shift Keying $m = 0.5$	(c) Tamed Freq. Shift Keying
$\frac{\omega T/2}{\sin(\omega T/2)}$ for $\lvert\omega\rvert \leq \frac{\pi}{T}$; 0 otherwise	(a') Fast Freq. Modulation	(b') Duobinary Freq. Modulation $m = 0.5$	(c') Tamed Freq. Modulation

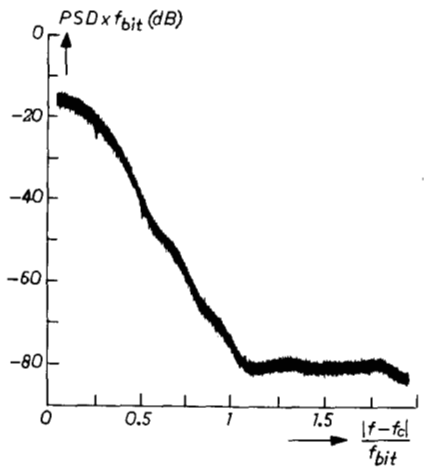

Fig. 17. Power spectral density function measured at the output of the TFM transmitter shown in Figs. 15 and 16, with 8-bit D/A converters, $L = 8$, truncation to $5T$ and $\alpha = 0$.

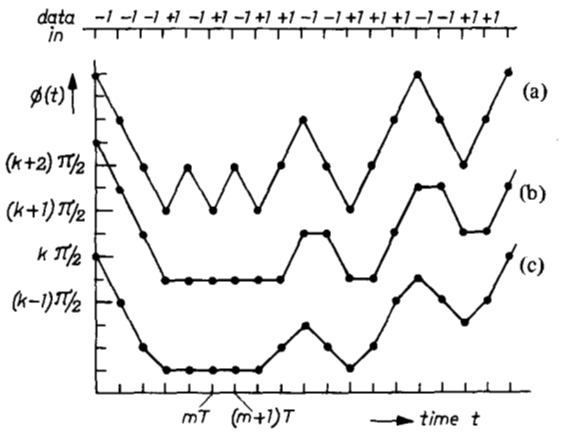

Fig. 18. Phase behavior of FFSK or MSK (a), Duobinary FSK with $m = 0.5$ (b) and Tamed FSK (c).

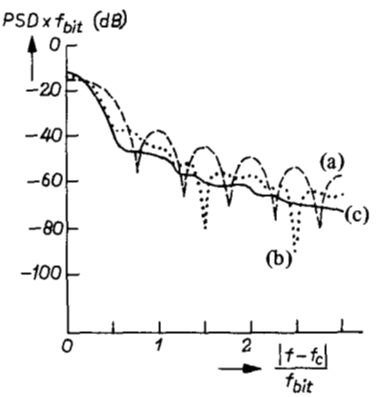

Fig. 19. PSDF's of FFSK or MSK (a), Duobinary FSK with $m = 0.5$ (b), and Tamed FSK (c).

ferent functions for $H(\omega)$ on the outgoing TFM spectrum has been investigated. In this section we compare the spectrum of TFM with spectra of other types of synchronous frequency modulation, which also exhibit a constant amplitude. Originally for $H(\omega)$ the function of equation (13) was used, giving rise to a continuous modulating signal. Now, for $H(\omega)$ a different function is chosen,

$$H(\omega) = [2 \sin(\omega T/2)]/(\omega T), \qquad -\infty < \omega < \infty \qquad (19)$$

producing a non-continuous modulating signal. In this case the impulse response $h(t)$ is of rectangular form and obviously satisfies the third Nyquist criterion. To clearly distinguish both cases, we talk about keying versus modulation (Table 1).

Several of these systems have been described in literature before, e.g., Fast Frequency Shift Keying [2, 3], Duobinary Frequency Shift Keying $m = 0.5$ [5, 11] and Duobinary Frequency Modulation $m = 0.5$ [5]***.

In Fig. 18 the phase behaviors for the three frequency shift keying systems are depicted for a certain data stream. In each of these systems the phase changes linearly with time between the transition points. The outgoing PSDF's of these systems are given in Fig. 19, showing a slight improvement in spectrum economy when a high-order correlative coding is used.

*** It should be noted that in literature the name Duobinary Frequency Modulation $m = 0.5$ does not uniquely define $H(\omega)$.

According to the classification of Kretzmer [12], several different functions for $S(\omega)$ can be taken, but only the three functions used give rise to a two-level eye opening if an orthogonal coherent demodulator is used as the receiver. The spectra of these three systems can be made much narrower, however, by the use of a filter $H(\omega)$ defined in relation (13). This is shown in Fig. 20.

CONCLUSION

In this paper we have described a novel and promising type of frequency modulation, named Tamed Frequency Modu-

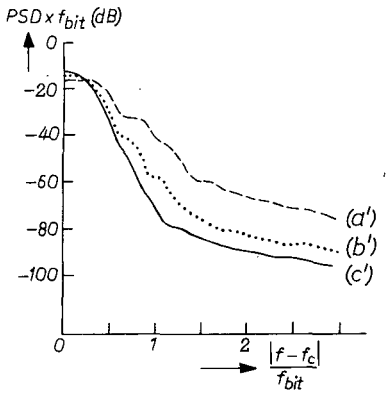

Fig. 20. PSDF's of Fast Frequency Modulation (a'), Duobinary Frequency Modulation with $m = 0.5$ (b') and Tamed Frequency Modulation (c'). In each system the truncation interval equals $5T$.

lation, for digital transmission. A very low out-of-band radiation is obtained as compared with other constant-envelope modulation techniques. In this way the severe constraints of the radio field can be met with the receiving filter shown in Fig. 12 and the PSDF of TFM in Fig. 3. For example, with a radio channel spacing of 25 kHz and a required data rate of 16 kbits/s the power radiated into the adjacent channel can be 85 dB lower than the power radiated into the wanted channel.

The detection quality is almost the same as for four-phase modulation.

Finally, it is shown that the implementation of the TFM transmitter and receiver can be relatively simple.

ACKNOWLEDGMENT

The authors would like to thank D. Muilwijk and B. van de Ham of Philips Telecommunication Industries for their contributions to the investigation.

REFERENCES

[1] R. W. Lucky, J. Salz, E. J. Weldon Jr., *Principles of Data Communication*, McGraw-Hill Book Company, New York, 1968.

[2] H. C. van den Elzen, P. van de Wurf, A Simple Method of Calculating the Characteristics of FSK Signals with Modulation Index 0.5, *IEEE Transactions on Communications*, vol. COM-20, No. 2, pp. 139-147, April 1972.

[3] R. de Buda, Coherent Demodulation of Frequency Shift Keying with Low Deviation Ratio, *IEEE Transactions on Communications*, vol. COM-20, No. 3, pp. 429-435, June 1972.

[4] F. Amoroso, Pulse and Spectrum Manipulation in the Minimum (Frequency) Shift Keying (MSK) Format, *IEEE Transactions on Communications*, vol. COM-24, No. 3, pp. 381-384, March 1976.

[5] G. J. Garrison, A Power Spectral Density Analysis for Digital FM, *IEEE Transactions on Communications*, vol. COM-23, No. 11, pp. 1228-1243, Nov. 1975.

[6] H. Nyquist, Certain Topics in Telegraph Transmission Theory, *AIEE Trans.*, vol. 47, pp. 617-644, April 1928.

[7] S. Pasupathy, Nyquist's Third Criterion, *Proceedings of the IEEE*, vol. 62, No. 6, pp. 860-861, June 1974.

[8] W. R. Bennett, J. R. Davey, *Data Transmission*, McGraw-Hill Book Company, 1965.

[9] A. D. Sypherd, Design of Digital Filters Using Read-Only Memories, *Proceedings of the NEC*, Chicago, vol. 25, 8-10 Dec. 1969, pp. 691-693.

[10] F. A. M. Snijders, N. A. M. Verhoeckx, H. A. van Essen, P. J. van Gerwen, Digital Generation of Linearly Modulated Data Waveforms, *IEEE Transactions on Communications*, vol. COM-23, No. 11, pp. 1259-1270, Nov. 1975.

[11] A. Lender, A Synchronous Signal with Dual Properties for Digital Communications, *IEEE Transactions on Communication Technology*, vol. COM-13, No. 2, pp. 202-208, June 1965.

[12] E. R. Kretzmer, Generalization of a Technique for Binary Data Communication, *IEEE Transactions on Communication Technology*, vol. COM-14, No. 1, pp. 67-68, Febr. 1966.

★

Frank de Jager was born in Amsterdam, The Netherlands, on June 13, 1919. He was graduated from the Technical University of Delft in 1946, when he joined the Philips Research Laboratories in Eindhoven and was assigned to the Telecommunications Department where he worked in the fields of carrier telephony, deltamodulation, vocoders, companders, data transmission, automatic equalization and, finally, in radio communication. In 1958 he received, together with Johannes A. Greefkes the Veder-Award for work on speech transmission with low signal-to-noise ratios. In 1972, together again with Johannes A. Greefkes, he received the 1972 IEEE Award in International Communication in honor of Hernand and Sosthenes Behn for contributions to communications systems research, in particular, for inventions in the delta-modulation area.

★

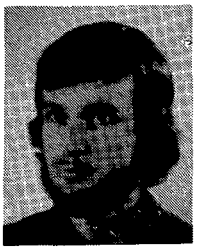

Cornelis B. Dekker (M'76) was born in The Netherlands, on May 23, 1950. He received the degree in electrical engineering from the Technical University, Delft, The Netherlands, in 1973.

After his military service he joined the Telecommunications Department of the Philips Research Laboratories where he is now working on digital communication via radio channels.

Mr. Dekker is a member of the Netherlands Electronics and Radio Society.